Available online at www.sciencedirect.com
SCIENCE DIRECT
Journal of Photochemistry and Photobiology A: Chemistry 177 (2006) 269–275
Journal of Photochemistry and Photobiology A:Chemistry
www.elsevier.com/locate/jphotochem

Transient IR absorption study of charge carriers photogenerated in sulfur-doped TiO_2

Kan Takeshita [a,*], Akira Yamakata [b,1], Taka-aki Ishibashi [b,2], Hiroshi Onishi [b,3], Kazumoto Nishijima [c], Teruhisa Ohno [c]

[a] *Mitsubishi Chemical Group Science and Technology Research Center Inc., 1000, Kamoshida-cho, Aoba, Yokohama 227-8502, Japan*
[b] *Surface Chemistry Laboratory, Kanagawa Academy of Science and Technology (KAST), KSP East 404, 3-2-1 Sakado, Takatsu, Kawasaki 213-0012, Japan*
[c] *Department of Material Science, Faculty of Engineering, Kyushu Institute of Technology, 1-1 Sensuicho, Tobata, Kitakyushu 804-8550, Japan*

Received 28 December 2004; received in revised form 5 April 2005; accepted 6 June 2005
Available online 14 July 2005

Abstract

Sulfur-doped TiO_2 was prepared by two methods; one was simple oxidation annealing of TiS_2, the other was mixing of titanium isopropoxide and thiourea. These two sulfur-doped TiO_2 preparations showed fairly different photocatalytic activity under visible light. The dynamics of photogenerated charge carriers were studied by the transient absorption measurement in the region of mid-IR. In both samples, excitation by 532 nm pulse led to photocarrier generation to the same extent. Nevertheless, the reactivity of the photocarriers was totally different. Photogenerated electrons and holes transferred to reactant gas in the latter sample, whereas they did not in the former sample. We attributed the different carrier behavior to the difference in the distribution of S atoms or particle size. These observations can explain the difference in capability of photocatalysis under visible light.

Keywords: Sulfur-doped titanium dioxide; Visible-light-response photocatalyst; Transient IR absorption; Photogenerated carriers

1. Introduction

Semiconductor-based photocatalysis is a promising technology that has a variety of applications. The applications range from air purification by decomposition of harmful organic compounds to energy generation by photoinduced water splitting into H_2 and O_2 [1–3]. Among many candidates, TiO_2 has proved to be the superior form of photocatalysis and has been widely utilized because of its high functionality, long-term stability and non-toxicity [4]. However, TiO_2 shows high reactivity only under ultraviolet light whose energy exceeds the band gap (3.2 eV for anatase crystalline phase). To make the best use of the solar spectrum, we need the development of photocatalysts that can yield high reactivity under visible light, and indeed, many researchers have tried to add visible light response to TiO_2.

One approach for acquiring a visible response is to introduce defects into the lattice through transition metals ion doping [5–7]. TiO_2 systems on which various photosensitizing dyes are adsorbed have also been widely investigated [8–10]. Recently, it has been reported that visible-light-response photocatalysts can also be produced by doping non-metal elements other than transition metals. For instance, nitrogen [11], sulfur [12] or carbon [13] doped TiO_2 were synthesized and they showed photocatalytic activity under visible light. Whether it is cationic or anionic, the doping of a foreign element into TiO_2 makes a donor or an acceptor level in the forbidden band and this level induces absorption of visible

* Corresponding author. Tel.: +81 45 963 3155; fax: +81 45 963 4261.
E-mail address: 5503103@cc.m-kagaku.co.jp (K. Takeshita).
[1] Present address: Catalysis Research Center, Hokkaido University, Sapporo 001-0021, Japan.
[2] Present address: Department of Chemistry, Graduate School of Science, Hiroshima University, Higashi-Hiroshima 739-8526, Japan.
[3] Present address: Department of Chemistry, Faculty of Science, Kobe University, Kobe 657-8501, Japan.

1010-6030/$ – see front matter © 2005 Elsevier B.V. All rights reserved.
doi:10.1016/j.jphotochem.2005.06.006

light. At the same time, however, this level may work as a carrier-recombination center, which decreases photocatalytic activity. Therefore, doping of a foreign element does not necessarily enhance response to visible light. To develop and improve visible-light-responsive photocatalysts, we should clarify what kind of doping or modification to TiO_2 is really effective in increasing activity under visible light.

Time-resolved infrared (TRIR) spectroscopy is a potential tool for this subject because it can give information of transient carriers in semiconductor photocatalysts. So far, several groups including us have applied this technique to reactions in oxidized semiconductors and related materials [14–20]. Electrons photoexcited in a semiconductor display structureless, monotonic absorption of IR light, which is attributed to transient absorption of electrons in conduction band or shallow midgap states [18,19]. The greatest advantage of employing IR light for probing is that the absorption signal from carrier electrons is not obstructed by other sources. Carrier electrons also give transient absorption in the visible region, but the bleach signal of catalysis itself or emission from excited catalysis falls on the target signal. For this reason, the IR region is more appropriate than the visible region for the present purpose. Another advantage of our TRIR measurement system is that we can detect minute absorption changes in a long time scale. This enables us to evaluate even slight differences in photocatalytic activity of carriers through small absorbance changes [18,19].

In the present study, we applied our TRIR system to sulfur-doped TiO_2 and investigated the dynamics of photogenerated charge carriers. We prepared sulfur-doped TiO_2 by two different methods. These two types of S-doped TiO_2 are interesting and are good models for examination because they have different forms of doping and fairly different photocatalytic activity under visible irradiation [12,21,22]. In the reference [12], S-doped TiO_2 was synthesized by oxidative annealing of TiS_2. The XPS measurement showed that S atoms were incorporated into the O site of TiO_2. On the other hand, in S-doped TiO_2 prepared by the method noted in references [21,22], S atoms substitute for some of the lattice Ti atoms. These studies indicate that forms of doping (e.g. oxidative number) are dependent on preparation conditions. Even more importantly, the difference of doping states has a strong influence on photocatalytic activity. Here we report the detailed dynamics of photogenerated holes and electrons in two types of S-doped TiO_2 and connect them with photocatalytic activity by use of a transient IR absorption study.

2. Experiment

In this study, we prepared sulfur-doped TiO_2 by two methods. In the first method, S-doped TiO_2 was synthesized by oxidation annealing of titanium disulfide (TiS_2) powder (High Purity Chemicals Laboratory Co., Ltd.) at 300–600 °C. In the second method, S-doped TiO_2 was prepared by mixing titanium isopropoxide and thiourea in ethanol, subsequent evaporation and calcination (under air at 500 °C). The details of each preparation procedure are shown in the literature [12,21,22]. After the preparation, S-doped TiO_2 powder was dispersed in water and spread on a CaF_2 plate. The density of the powder was 1–1.5 mg/cm^2.

Time resolved infrared absorption measurement was conducted using systems similar to those previously reported [23,24]. For an excitation pulse, we used the second (532 nm) or third (355 nm) harmonics of Q-switched Nd:YAG laser (10 ns pulse). The excitation pulse energy was 0.2–2 mJ/cm^2 and the repetition rate was 0.03–10 Hz. A probe light (emitted from the glober source) was focused on the sample plate with an ellipsoidal mirror. The transmitted light was dispersed in a monochromator of 50 cm focal length and the monochromatic output was detected by an mercury–cadmium–telluride (MCT) detector. The MCT output was amplified in AC-coupled amplifiers and accumulated in a digital sampling oscilloscope as a function of delay time at a fixed wavelength. Temporal profiles were reconstructed to transient IR absorption spectra at different delay times. The time-resolution was about 50 ns, which was determined by the response of the detector. Time-resolved infrared absorption was measured at room temperature under vacuum or desired gas reactants.

The photocatalytic activity of S-doped TiO_2 was characterized in terms of the degradation of an organic dye, methylene blue. Briefly, 100 mg of each photocatalyst was suspended in 5 ml of methylene blue aqueous solution (50 mmol dm^{-3}). The solution was stirred in the absence of light to attain the equilibrium adsorption on the catalyst surface. The solution was then irradiated during stirring for 10 min using a 1000 W Xe lamp. The short-wavelength components of the light were removed by cutoff glass filters. The extent of dye photodecomposition was estimated by measurement of the UV–vis absorption spectrum.

3. Results

3.1. Characteristics and photocatalytic activity of S-doped TiO_2

In the first method of preparing sulfur-doped TiO_2, we followed the same procedure reported by Umebayashi et al. [12]. We measured the absorption (diffuse reflectance) spectra and the photocatalytic activity of the sulfur-doped TiO_2 prepared in this method. The results shown below were in good agreement with their results. Here, we briefly state the characteristics of this sample showing their and our results.

When TiS_2 powder is calcined under air, sulfur atoms in TiS_2 are gradually replaced by oxygen atoms. In this process, we can control content of sulfur atoms by varying calcination temperature and time. Fig. 1 shows the change of absorption spectrum of TiS_2 by calcination under air, at 300 °C for 30 min, at 500 °C for 30 min, or at 600 °C for 2 h. This spectrum suggests that most parts of TiS_2 powder remained unchanged at 300 °C but that it was nearly completely trans-

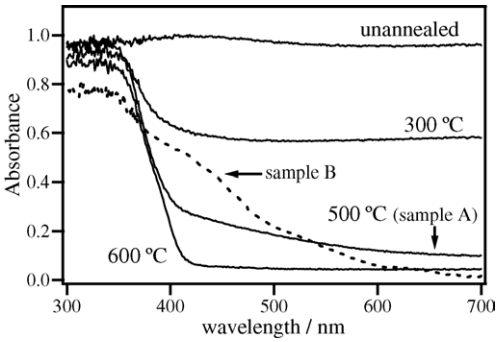

Fig. 1. Diffuse reflectance spectra of TiS_2 annealed at 300 °C, at 500 °C, or at 600 °C, and unannealed TiS_2. Spectrum of S-doped TiO_2 sample B is also shown for the comparison.

formed into TiO_2 at 600 °C. Annealed at 500 °C, most of sulfur atoms are substituted by oxygen atoms, but some of sulfur atoms remain unchanged. This is why the sample annealed at 500 °C had absorption in the visible region. Umebayashi et al. confirmed this structure by X-ray diffraction (XRD) analysis and X-ray photoelectron spectroscopy (XPS). We refer to TiS_2 powder annealed at 500 °C as the 'S-doped TiO_2 sample A' hereafter.

We also prepared S-doped TiO_2 from titanium isopropoxide and thiourea. Some of the authors have previously reported the characteristics of this sample, such as UV–vis absorption and XPS spectrum [21]. In this work, we call this sample the 'S-doped TiO_2 sample B'. The atomic content of S atom in sample B has been reported as 0.5–1.6% [21]. In addition, we presume that the S atom content in sample A is roughly the same as sample B because both sample A and B absorb visible light to the same extent.

The photocatalytic activity of the S-doped TiO_2 samples A and B was evaluated by measuring the decomposition rates of methylene blue in aqueous solution. The results are shown in Fig. 2. Both samples A and B showed strong activity under UV irradiation. However, response to visible light was considerably different between samples A and B. Sample A had only a little activity under visible irradiation, whereas sample B showed fairly large activity.

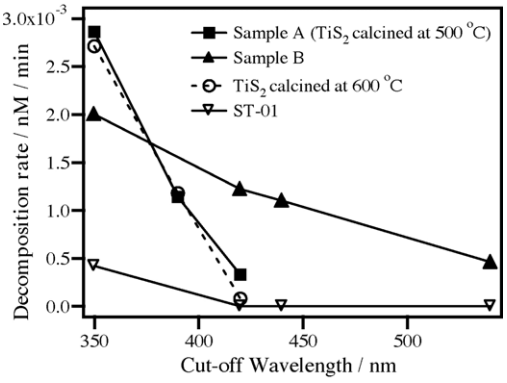

Fig. 2. Photocatalytic activity of the S-doped TiO_2 samples A and B, which was evaluated by decomposition rates of methylene blue. The horizontal axis represents 'cut-off wavelength' for irradiation of white light from a Xe lamp. (For example, '420 nm' means that wavelength shorter than 420 nm was cut.) Photocatalytic activity of the standard TiO_2 (ST-01, Ishihara Sangyo) and TiS_2 annealed at 600 °C are also shown for the comparison.

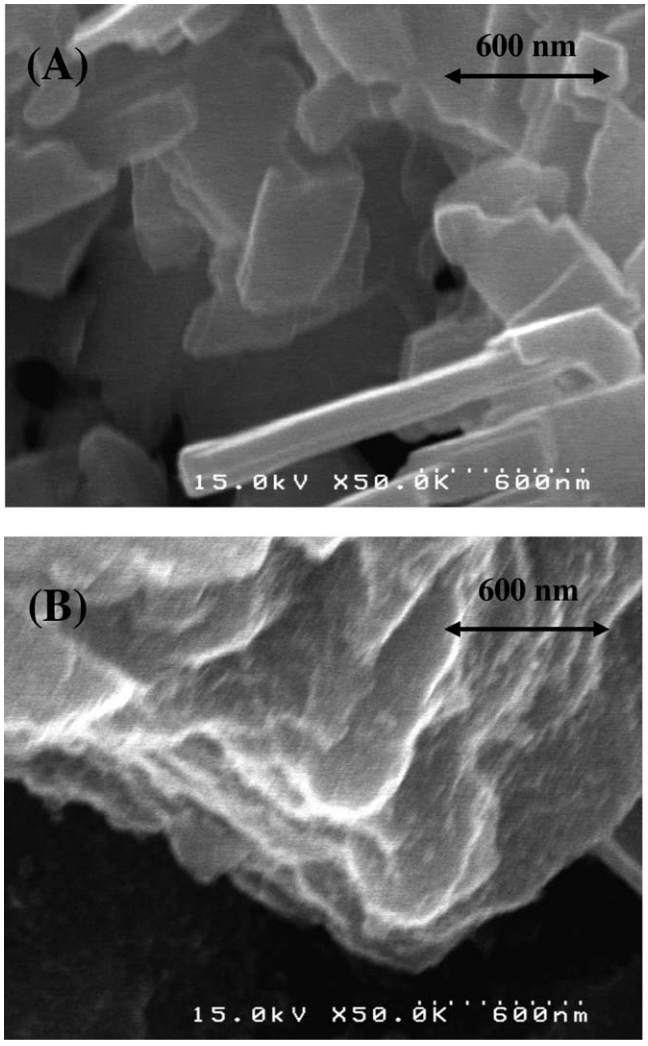

Fig. 3. S.E.M. images of S-doped TiO_2 samples A and B.

Fig. 3 presents SEM images of sample A and B. A particle of sample A had a diameter of 1–2 μm, which was derived from the start material–TiS_2 powder. The particle size of sample B could not be estimated from the Fig. 3B, which means the particles of sample B were much smaller than sample A. It is known that the particle size of TiO_2 synthesized from titanium isopropoxide is tens of nanometers [8]. Presumably, S-doped TiO_2 sample B has a similar particle size.

3.2. Transient absorption spectra and decay

Fig. 4A depicts transient absorption spectra of S-doped TiO_2 sample A in the mid-IR region when it was excited by ultraviolet (355 nm) or visible (532 nm) pulse. These spectra were measured in the atmosphere. In both excitation wavelengths, we observed broad unstructured transient absorption spectra that monotonously increased in intensity

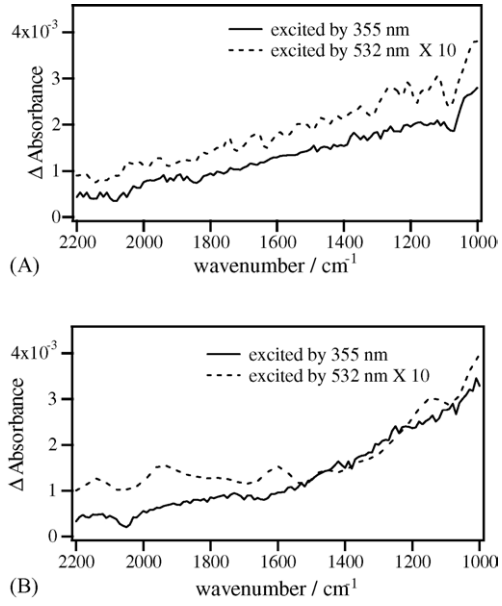

Fig. 4. Transient absorption spectra of S-doped TiO_2 samples A and B in the mid-IR region at 1 μs after pulse excitation.

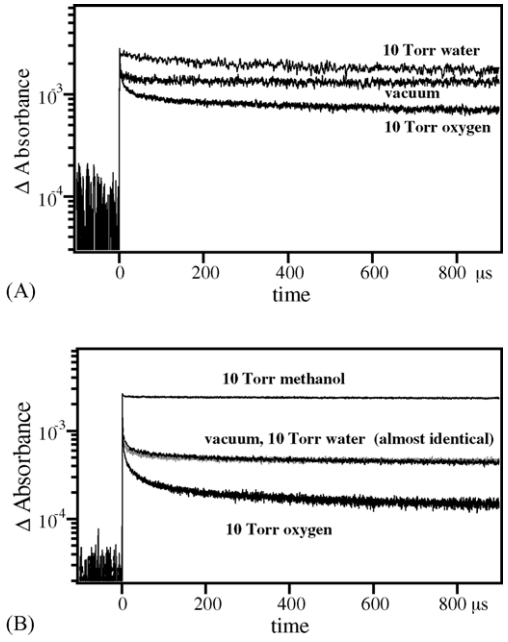

Fig. 5. Comparison of the decay of the transient absorption at 2000 cm^{-1} under various gas reactants. Excitation wavelength was 355 nm. A and B show the signals for samples A and B, respectively.

with decreasing wave number. This absorption is attributed to the intra-band transition of free electrons in the conduction band and optical transitions of trapped electrons from shallow midgap states to the conduction band [18]. Although the relative intensity of the transient absorption was considerably different between 355 and 532 nm excitation, the shape of the spectrum was almost identical. These observations show that free charge carrier generation occurred not only by 355 nm light excitation but also by 532 nm light excitation. However, the quantity of charge carrier generation was much larger by 355 nm light than by 532 nm light.

The transient absorption spectra for S-doped TiO_2 sample B are shown in Fig. 4B. Again, the excitation wavelength was 355 or 532 nm. We observed the same broad unstructured transient absorption as we observed in sample A. The difference in the shape and intensity of the spectra by the excitation wavelength was nearly the same as that observed in sample A.

The decay measurement and analysis of the transient absorption under various gas reactants are helpful in investigating the kinetics of photogenerated carriers in these samples [19]. Fig. 5A and B show the decay of transient absorption at 2000 cm^{-1} after 355 nm pulse excitation for S-doped TiO_2 samples A and B, respectively. The measurements were conducted in the presence of 10 Torr oxygen, water vapor, or methanol vapor. Measurements under vacuum conditions were also conducted for reference. In sample A, the decay was accelerated by the presence of oxygen, whereas it was decelerated by water vapor. Electrons are consumed by recombination with holes and also by reactions with adsorbates [19,20]. Therefore, the oxygen-induced quench is ascribed to the reaction of electrons with adsorbed oxygen. On the other hand, the deceleration of decay by water vapor can be explained by the quenching of the hole. Holes photogenerated in the valence band of TiO_2 oxidize water to oxygen [2,4]. In this experimental condition, it is considered that hydroxyl anions effectively capture the holes in the initial step of the oxidation.

Although these acceleration and deceleration behaviors were in good agreement with the result of the same experiments for TiO_2 or Pt/TiO_2 [19] in sample A, the situation was somewhat different in sample B. Oxygen accelerated the signal decay as it did in sample A, but deceleration by water did not occur. This fact means that holes photogenerated in sample B did not have the ability to oxidize water. We also measured transient absorption under methanol vapor, because alcohol such as methanol is known as a strong scavenger of holes. The result is also shown in Fig. 5B. As expected, the decay was decelerated because of quenching of the holes by methanol vapor. The difference in the reactivity between water and methanol can be explained as follows. The edge of the valence band of TiO_2 is at 3.0 eV versus normal hydrogen electrode (NHE). This level is enough for oxidation of water. However, if holes are captured by deep trap sites, holes may lose the high potential for oxidation of water. The oxidation potential of water is about 1.2 eV. In reality, however, considerable amount of excess energy is required to oxidize water because of the presence of an overpotential [2–4]. Therefore, the level of deep trap sites is probably inadequate for oxidation of water. On the other hand, the oxidation potential of methanol is about 0.6 eV. Hence, oxidation of methanol is much easier than oxidation of water. From the results shown in Fig. 5B, we can presume holes generated by UV irradiation will be soon captured by deep trap sites in sample B.

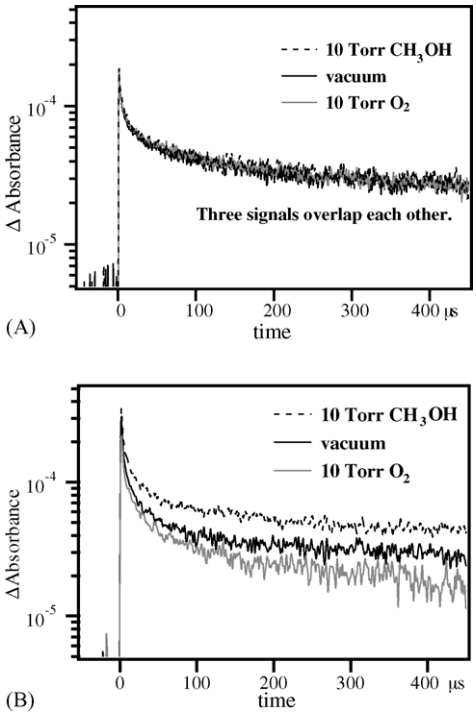

Fig. 6. Comparison of the decay of the transient absorption at 2000 cm^{-1} under various gas reactants. Excitation wavelength was 532 nm. A and B show the signals for samples A and B, respectively.

The trapped holes cannot oxidize water, but they can oxidize methanol. The further discussion will be described in the Section 4.

The results shown in Fig. 5A and B explain the activity of each photocatalyst under ultraviolet light. As a whole, both samples A and B had photocatalytic activity under UV light, although the activity of sample B was smaller than sample A. We next conducted the same experiment using 532 nm pulse light excitation to examine the activity under visible light. We present the results in Fig. 6A and B. The decay features were considerably different between ultraviolet and visible excitation. First of all, in sample A, the decay was hardly affected by gas reactants. This result indicates that electrons and holes generated by visible light excitation did not move to gas reactants. In sample B, the decay was accelerated by oxygen and decelerated by methanol, but the extent of rate changes was rather smaller than observed by ultraviolet excitation. This fact means that electrons and holes are less able to move to reactants by visible excitation than by UV excitation.

In terms of photocatalytic activity, the results shown in Fig. 6A and B proved that sample A did not work as photocatalysis under 532 nm light, but that sample B worked even under 532 nm light. This is correlated to the photocatalytic feature shown in Fig. 2, and a detailed interpretation will be given in the next section.

Fig. 7 shows the initial intensity of the transient absorption of S-doped TiO_2 samples A, B, and TiS_2 annealed at 600 °C. TiS_2 powder annealed at 600 °C gave only a tiny transient absorption with the irradiation of 532 nm light because it

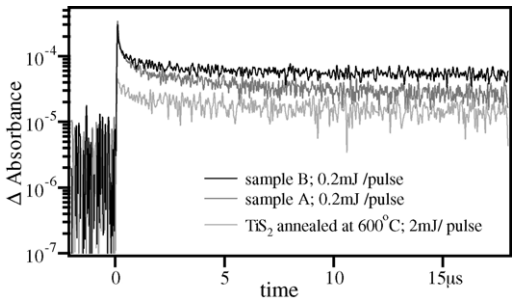

Fig. 7. Comparison of the initial intensity of the transient absorption among S-doped TiO_2 samples A, B, and TiS_2 annealed at 600 °C. Excitation wavelength was 532 nm.

has almost no absorption at this wavelength. (The spectrum shown in Fig. 1 indicates that TiS_2 was almost completely transformed into TiO_2 at this temperature.) The initial intensities of transient absorption observed for samples A and B were nearly the same, and they were 10 times as large as that observed for TiS_2 annealed at 600 °C, regardless of 1/10 excitation pulse energy. Since the initial intensity of transient absorption reflects the quantity of photogenerated electrons, this result means that photocarrier generation in samples A or B was about 100 times as frequent as that in TiS_2 annealed at 600 °C. It is interesting that photo carrier generation occurred to the same extent in both samples A and B, but the mobility of the photocarriers was considerably different.

4. Discussion

In this section, let us discuss the differences in photocatalytic activity between S-doped TiO_2 samples A and B. Photoexcitation of samples with light of an energy that matches the band gap yields electron-hole pairs. Photogenerated electrons and holes can migrate to the surface and react with adsorbed reactants, or they may undergo undesired recombination. The photocatalytic efficiency depends on the competition between these two processes, that is, the ratio of reaction to recombination. The ratio of reaction to recombination depends on the electronic properties of the photocatalyst (e.g. energy level of CB, VB, and trap states). Therefore, to discuss the differences in photocatalytic efficiency, we first consider the electronic properties of S-doped TiO_2.

TiO_2 has a wide band gap of 3.2 eV in the anatase crystalline phase. The edge of the valence band is at 3.0 eV versus NHE. The conduction band minimum is located at −0.2 eV versus NHE. Doping of the S atom perturbs CB or VB (or both of them), and produces states in the band gap of TiO_2 that absorb visible light (Fig. 8). Umebayashi et al. analyzed the band structures of S-doped TiO_2 by ab initio calculation [12,22]. According to their calculation, an electron-occupied level appears slightly above the VB, which contributes to visible absorption. The edge of the valence band is at roughly 2.0 eV versus NHE. Such band formation is possible if the

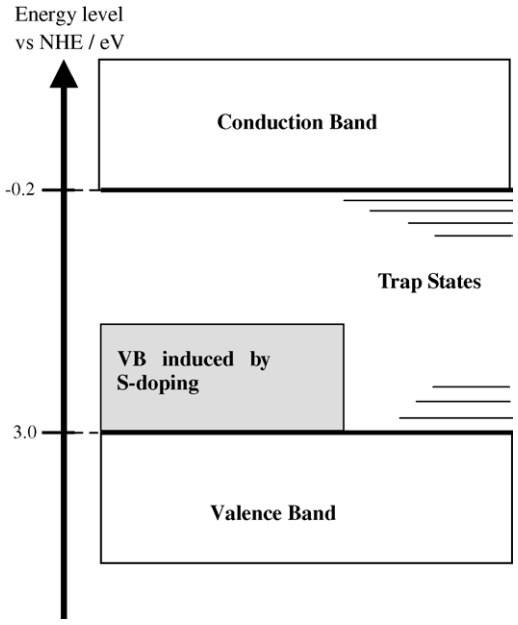

Fig. 8. Estimated energy diagram of S-doped TiO_2.

quantity of doped S atom is adequate. If the quantity of S atoms is very small and S doped sites are isolated in bulk TiO_2, the doped S atom works as a trap state, like a 'defect'. The different preparation methods between samples A and B might affect the form of band and trap formation.

We here propose the following presumption to explain the difference of photocatalytic activity; the distribution of S atoms is different between samples A and B (Fig. 9). In sample A, S atoms exist mainly in the central part of particles. In sample B, on the other hand, the distribution of S atoms is rather uniform, which means S atoms also exist near the surface. These different distributions of S atoms are easily inferred from each preparation method. Sample A is synthesized by annealing of a TiS_2 particle. In the annealing process, firstly O atoms replace S atoms near the surface. Then this replacement gradually spreads to the inner part of the particle. Consequently, the core of the particle has a larger content of S atoms than the surface. Meanwhile, S atoms derive from thiourea in sample B. Hence S atoms must exist near the surface to a certain extent. Although these assumptions are currently rather speculative, they can well explain the experimental results as shown below.

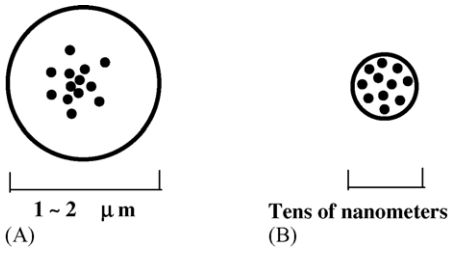

Fig. 9. Proposed difference in distribution of S atoms in S-doped TiO_2 samples A and B (dots represent doped S atoms).

Before explaining photocatalytic reactions under UV and visible light, we here describe states in an S-doped TiO_2 particle as the following four distinctive sites:

(i) A site that can absorb 355 nm light (unperturbed TiO_2).
(ii) A site that can absorb 532 nm light (induced by doping of S atoms).
(iii) A trap site that can catch photogenerated holes (induced by doping of S atoms).
(iv) A reaction site.

The distribution of these (i)–(iv) sites should be determined by the distribution of S atoms. Now we are ready to explain the different behaviors of photogenerated carriers between samples A and B. The discussion is developed below.

Fig. 5 shows the activity of the carriers under UV irradiation. Near the surface, a particle of sample A has almost the same structure as TiO_2. Most parts of UV light are absorbed in the proximity of the surface. Accordingly, the activity of photogenerated carriers is the same as those in pure TiO_2. Meanwhile, a particle of sample B has trap states (site iii) near the surface, so that the activity of carriers is different from carriers in pure TiO_2. UV light irradiation generates holes in the valence band and these holes are eventually captured by the trap states. Once the trap sites catch holes, holes lose the high potential for oxidation of water. This difference in the reactivity of holes with water clearly appears in Fig. 5A and B. A large amount of energy is required to oxidize water because of the presence of an overpotential. The experimental results indicate that the holes photogenerated in sample B do not have enough energy to oxidize water or hydroxyl anion. However, they can oxidize methanol (Fig. 5B) and methylene blue (Fig. 2). Methanol strongly adsorbs on the photocatalyst surface as a methoxy species. This fact means that methanol can be oxidized through direct hole transfer from the photocatalyst without a hydroxyl radial [20]. In terms of the oxidation potential, the energy required for the oxidation of methanol is smaller than that required for the oxidation of water. Taking these facts into consideration, it is not strange that holes photogenerated in sample B, which do not have enough energy to oxidize water, can oxidize methanol. The oxidation of methylene blue can also be explained by the direct hole transfer. In addition, the experiment shown in Fig. 2 was conducted in the solution condition, where some species other than a hydroxyl radical may relate to oxidative decomposition.

Fig. 6 shows the activity of the carriers under visible irradiation. In sample A, most of site (ii), which absorbs visible light, is located at the center of the particle. Therefore, with visible irradiation, free carriers are generated mainly in the core of the particle. These carriers disappear through a recombination process in the semiconductor particle before migrating to outside gas reactants. This means that the existence of gas reactants has almost no influence on the decay process of free electrons. This presumption is supported by the experimental results shown in Fig. 6A. On the other hand,

in sample B, site (ii) is distributed also on the surface. Carriers generated by visible excitation in site (ii) can move to site (iv), where a gas reactant extracts a carrier from the photocatalyst.

Another possible reason for the difference in activity between samples A and B is the difference in particle size. The S.E.M. images of samples A and B (Fig. 3) showed that the diameter of the sample A particle was 1–2 μm and that the diameter of the sample B particle was far smaller than sample A (tens of nanometers). In sample A, electrons and holes generated in the core of the particle disappear through recombination before migrating to the surface, whereas, in sample B they can reach the surface because of the short migration path length. This assumption can also explain the difference of photocatalytic efficiency under visible light, together with the difference in the distribution of S atoms as mentioned above.

5. Summary

We investigated the behaviors of photogenerated charge carriers in two types of sulfur-doped TiO_2 (samples A and B) by transient absorption measurement in the region of mid-IR. The activity of photocarriers was fairly different between these two samples. In sample A, the behavior of the UV-light-generated electrons and holes was in good agreement with the result of the same experiments for pure TiO_2. On the other hand, in sample B, UV-light-generated holes did not have the ability to oxidize water, which is related to the existence of trap states near the surface. Excitation by 532 nm pulse led to photocarrier generation to the same extent in both samples. However, the reactivity of the photocarriers was totally different. Photogenerated electrons and holes migrated to reactant gas species in sample B, whereas they did not in sample A. We explained all these experimental results by the difference in the distribution of S atoms or the particle size.

Acknowledgments

This work was supported by Grants-in-Aid for Scientific Research on Priority Areas (417) and Exploratory Research (No. 15655077) from the Ministry of Education, Culture, Sports, Science and Technology of the Japanese Government, and also Core Research for Evolutional Science and Technology by Japan Science and Technology Agency.

References

[1] A. Fujishima, K. Honda, Nature 37 (1972) 238.
[2] M.A. Fox, M.T. Dulay, Chem. Rev. 93 (1993) 341.
[3] A. Heller, Acc. Chem. Res. 28 (1995) 503.
[4] M.R. Hoffmann, S.T. Martin, W. Choi, D.W. Bahnemann, Chem. Rev. 95 (1995) 69.
[5] A.K. Ghosh, H.P. Maruska, J. Electrochem. Soc. 124 (1977) 1516.
[6] W. Choi, A. Termin, M.R. Hoffmann, J. Phys. Chem. 98 (1994) 13669.
[7] M. Anpo, Catal. Surv. Jpn. 1 (1997) 169.
[8] B. O'Regan, M. Grätzel, Nature 353 (1991) 737.
[9] Y. Tachibana, J.E. Moser, M. Grätzel, D.R. Klug, J.R. Durrant, J. Phys. Chem. 100 (1996) 20056.
[10] R. Abe, K. Hara, K. Sayama, K. Domen, H. Arakawa, J. Photochem. Photobiol. A Chem. 137 (2000) 63.
[11] R. Asahi, T. Morikawa, T. Ohwaki, K. Aoki, Y. Taga, Science 293 (2001) 269.
[12] T. Umebayashi, T. Yamaki, H. Itoh, K. Asai, Appl. Phys. Lett. 81 (2002) 454.
[13] H. Irie, Y. Watanabe, K. Hashimoto, Chem. Lett. 32 (2003) 772.
[14] T.A. Heimer, E.J. Heilweil, J. Phys. Chem. B 101 (1997) 10990.
[15] H.N. Ghosh, J.B. Asbury, T. Lian, J. Phys. Chem. B 102 (1998) 6482.
[16] H.N. Ghosh, J.B. Asbury, Y. Weng, T. Lian, J. Phys. Chem. B 102 (1998) 10208.
[17] J.B. Asbury, E. Hao, Y. Weng, T. Lian, J. Phys. Chem. B 104 (2000) 11957.
[18] A. Yamakata, T. Ishibashi, H. Onishi, Chem. Phys. Lett. 333 (2001) 271.
[19] A. Yamakata, T. Ishibashi, H. Onishi, J. Phys. Chem. B 105 (2001) 7258.
[20] A. Yamakata, T. Ishibashi, H. Onishi, J. Phys. Chem. B 107 (2003) 9820.
[21] T. Ohno, T. Mitsui, M. Matsumura, Chem. Lett. 32 (2003) 364.
[22] T. Ohno, M. Akiyoshi, T. Umebayashi, K. Asai, T. Mitsui, M. Matsumura, Appl. Catal. A 265 (2004) 115.
[23] K. Iwata, H. Hamaguchi, Appl. Spectrosc. 44 (1990) 1431.
[24] T. Yuzawa, C. Kato, M.W. George, H. Hamaguchi, Appl. Spectrosc. 48 (1994) 684.